

# Fourier Transform Near-Infrared Monitoring of Reacting Resins Using an Evanescent Wave High-Index Fiber-Optic Sensor

JOY P. DUNKERS,\* KATHLEEN M. FLYNN, MITCHELL T. HUANG, and WALTER G. McDONOUGH

*Polymers Division, National Institute of Standards and Technology, Quince Orchard and Clopper Roads, Gaithersburg, Maryland 20899*

In this work, a high-index silica-based fiber-optic mini-bundle sensor was constructed and implemented with a Fourier transform near-infrared spectrometer in the spectral region from 10 000 to 4500  $\text{cm}^{-1}$ . The refractive index of the multimode step index fiber was 1.618. This arrangement allows the propagation of waveguiding modes when the sensor is immersed in most resin systems. The reactions of a polyisocyanurate resin system and an epoxy resin system were monitored and peak assignments were made and discussed with respect to their potential for use in real-time analysis to be applied to cure control. Last, cure monitoring with this sensor was successfully demonstrated in a glass-reinforced resin transfer molded epoxy part.

Index Headings: Near infrared; Fiber optics; Composite; Cure; Epoxy; Polyisocyanurate.

## INTRODUCTION

The issue of part-to-part variability in manufacturing has been a problem that has plagued the composites industry for many years, and a large effort is being made not only to monitor but also to control the variability. There can be multiple causes of part nonuniformity that include incomplete mold filling, void formation, preform deformation, and cure variability. Cure variability can be categorized as cure nonuniformity between parts or within a part. It is the focus of this work to demonstrate the feasibility of using near-infrared (NIR) spectroscopy and fiber optics to monitor the cure within the resin or composite rather than at its surface. Future efforts will focus on integrating the cure data with the process control computer to achieve feedback control for resin transfer molding (RTM) as in previous work.<sup>1</sup>

Near-infrared spectroscopy has been widely used in process monitoring not only in polymer science<sup>2,3</sup> but also in the agriculture and food processing,<sup>4</sup> pharmaceutical,<sup>5</sup> and petro-chemical industries.<sup>6</sup> The vast majority of the remote analyses on polymer systems were done with transmission probes.<sup>7,8</sup> In the composites industry, it is desirable to have knowledge of the cure in the center thickness of the part, since reaction exotherms may cause substantially different curing between the part center and surface. Cure monitoring deep inside a composite necessitates the use of a fiber-optic sensor that is noninvasive enough to be incorporated into the final part. A fiber-optic sensor based on evanescent wave spectroscopy can be incorporated into a mold without disturbing the preform

or affecting the final composite properties. Considering the current state of composite manufacturing, it is not feasible to incorporate the sensor into every part or even a few select parts. The requirements for incorporating a sensor are rather rigid. The sensor system must adapt to the current mold because of the enormous cost of retooling molds. Rather, it is envisioned that the cure sensor could be used in low-volume, proto-type manufacturing laboratories that are precursors to the high-volume operations to establish cure schedules and do quality-control checks.

Evanescent wave fiber-optic spectroscopy relies on the fact that the guiding medium maintains a higher refractive index than the surrounding medium. A review of the theory of evanescent wave phenomena in fibers has been previously presented.<sup>9</sup> A commercial silica fiber optic ( $n = 1.45$ ) has a lower refractive index than most resin systems of interest and is thus not suitable for waveguiding experiments. However, near-infrared evanescent wave sensing has been accomplished by using a commercial-grade silica fiber optic and a specialty fluorinated epoxy resin having a refractive index lower than that of the silica fiber.<sup>10</sup> This work uses a fiber with  $n_D = 1.618$ . Evanescent wave sensing has been previously demonstrated with this silica/lead oxide fiber by using the shift in fluorescence emission as a means to follow the cure of an epoxy.<sup>11</sup>

In this work, cure sensing of a fast reacting polyisocyanurate resin was demonstrated. Also, cure sensing of a resin transfer molded epoxy composite was performed with the sensor embedded into the center of the composite thickness. Peak assignments and conversion curves will be presented. In addition, an effort will be made to identify potentially useful peaks for cure sensing and control for the resin systems. Further development of this sensing system hinges on making the optics more rugged. More importantly, a better signal-to-noise (S/N) ratio can be achieved by use of better quality, commercially drawn, high-index fibers. It may then be possible to use a single fiber. Commercial fibers with the desired step refractive index profile do not exist off the shelf, but can be specially drawn.

## EXPERIMENTAL

The polyisocyanurate resin used is being considered by the automotive industry for use in structural applications because of its high-temperature properties. The isocyanate was Spectrim MM 364-A (Dow Chemical Com-

Received 26 March 1997; accepted 4 November 1997.

\* Author to whom correspondence should be sent.

pany)<sup>†</sup> and consisted of diphenylmethane diisocyanate (MDI) (64–74%), MDI homopolymer (15–30%), and catalyst (5–10%). The polyol was Spectrim MM 364-B, a polyether polyol blend. The catalyst used was Dabco 33-LV (Air Products and Chemicals, Inc.), and is a mixture of 1,4-diazabicyclo(2,2,2)octane (33%) and dipropylene glycol (67%).

A manual mixing method for this experiment (components supplied by Ellsworth Adhesive Systems) was employed, utilizing an apparatus resembling a modified caulking gun. First, the isocyanate resin was poured into one plastic chamber that had an end cap inserted on its outlet port. Subsequently, the catalyst at 0.385 wt % was added into the polyol (in a beaker) and was mixed with the polyol for 30 s. Then the mixture was poured into another end-capped chamber. Larger caps were then attached to the other ends of the chambers. The volumetric ratios of the chambers resulted in a volume ratio of 2:1 isocyanate to polyol. The chambers were then placed inside the modified caulking gun with the plungers attached to the large end of the chambers. The gun was then positioned so that the resin was not near the outlet ports, and the outlet caps were removed. Subsequently, a static mixer was attached to outlets of the two chambers. The entire apparatus was then brought near the 14 cm path-length sample cell. A flexible tube was then attached to the end of the static mixer, and the other end of the tube was positioned over the mold cavity. The isocyanate and polyol were subsequently forced through the static mixer and into the sample cell that was preheated to 55 °C. In addition, triallyl-1,3,5-triazine-2,4,6-(1H,3H,5H)trione (98%) and diphenylmethane diisocyanate were purchased from Aldrich and used as received for NIR model compounds.

The epoxy resin system consisted of a diglycidyl ether of Bisphenol A (DGEBA) monomer (Tactix 123, Dow Chemical Company) and two amines. Aromatic methylene dianiline (MDA) and aliphatic poly(propylene glycol)bis(2-aminopropyl ether) (D400) ( $M_n \sim 400$ ) were purchased and used as received from Aldrich. The epoxy/amine stoichiometry is 2 mol oxirane/1 mol amine. The amine composition consisted of 0.75 mol MDA and 0.25 mol D400. For the curing experiments, the MDA was melted (mp 89–90 °C). To the melted MDA, the room-temperature DGEBA monomer was added and stirred until homogeneous. After the mixture was cooled to about 50 °C, the D400 component was added and stirred until homogeneous. The mixture was then poured into the room-temperature RTM pressure pot. The details of the resin transfer molding system have been previously described.<sup>12</sup> The mold was filled with a random glass mat, and the sensor exposure length was 14 cm. The epoxy was degassed at –103 kPa for 10 min prior to mold filling, and the mold wall temperature was monitored.

The Fourier transform infrared (FT-IR) spectrometer was a Nicolet Magna 550 equipped with a quartz–tungsten–halogen white light source, calcium fluoride beam-splitter, and a mercury–cadmium–telluride (MCT-A) de-

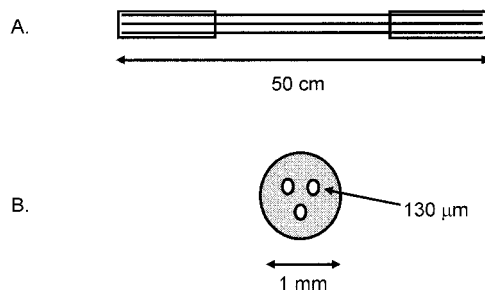


FIG. 1. Schematic diagram of the high-index fiber-optic mini-bundle sensor. (A) Side view; (B) end-on view.

tor. Future experiments will be performed with an InSb detector. For the epoxy resin system, spectral acquisition and delay time were automated with the use of a programmed macro. One hundred scans were coadded at a resolution of 16  $\text{cm}^{-1}$  by using the Omnic 3.1 software with a time delay of 5.7 min. Each spectrum took 36.5 s to acquire at a mirror velocity of 1.90 cm/s. For the polyisocyanurate resin system, the spectral acquisition and delay time were automated by using the RapidScan software. Fifty scans were coadded at a resolution of 16  $\text{cm}^{-1}$  with a 30 s delay time, and each spectrum took 4.44 s to acquire at a mirror velocity of 3.16 cm/s.

The sensor was constructed by using a mini-bundle of multiple fiber optics to promote signal-to-noise by increasing the energy throughput. After the fibers were cleaved to a length of 50 cm, the fiber ends were glued into a nylon tube with fast curing epoxy. The ends were then polished to be free of defects when inspected visually. The sensor in Fig. 1 consists of three 130  $\mu\text{m}$  diameter high-refractive-index silica fibers doped with lead oxide. The composition of the fibers is 46.0%  $\text{SiO}_2$ , 45.3%  $\text{PbO}$ , 5.6%  $\text{K}_2\text{O}$ , 2.5%  $\text{Na}_2\text{O}$ , and 0.6%  $\text{R}_2\text{O}_3$  where  $R$  represents the remaining substituents.<sup>13</sup> The doping of the silica fiber raises the refractive index ( $n$ ) to 1.612, which enables waveguiding for most resin systems. This refractive index was measured by using a white light source and index matching fluids and compared to the quoted value of 1.618 ( $n_D$ ).<sup>14</sup>

## RESULTS AND DISCUSSION

It is worthwhile to mention the benefits and detriments when selecting a fiber sensor and resin system. It is well understood that one of the difficulties of NIR spectroscopy is the intrinsically low absorptivities. In fact, the absorbance is approximately one order of magnitude lower than its mid-infrared counterpart,<sup>15</sup> which leads to problems in obtaining an acceptable signal-to-noise ratio. There are a number of ways to maximize S/N, and one is to increase the number of scans taken. There are limitations to this approach when a reacting system is studied because of the need for time resolution. It is also desirable to maximize the absorbance intensity to increase S/N. One way to do this is to increase the exposure length. However, the practicality of the situation must be considered, since we are working in a prototype manufacturing rather than a laboratory environment and understand that the fiber exposure length is limited by the mold size. Last, matching closely the refractive indices of the fiber and resin will increase the peak intensities by increasing the

<sup>†</sup> Identification of a commercial product is made only to facilitate experimental reproducibility and to adequately describe experimental procedure. In no case does it imply endorsement by NIST or imply that it is necessarily the best product for the experimental procedure.

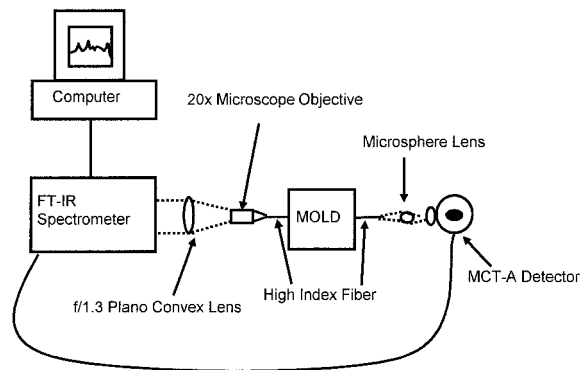


FIG. 2. Schematic diagram of FT-NIR setup. The mold is attached to the RTM equipment, not shown.

depth of penetration ( $d_p$ ) of the evanescent field. With an increase in the  $d_p$ , the energy throughput decreases. Therefore, the desired time resolution for the reacting system, the fiber exposure length, and the index matching of the fiber and resin throughout the reaction must all be considered to optimize S/N by balancing absorbance intensity and energy throughput.

Figure 2 is a schematic diagram of the integration of the fiber optic protruding from the mold and the rest of the system consisting of the Fourier transform infrared spectrometer and additional optics. As is clear from this figure, the light is directed out of the side of the spectrometer and through a 7.5 mm diameter,  $f/1.3$  plano convex lens that has a large aperture for condensing the large collimated beam exiting the side of the spectrometer. A microscope 0.40 numerical aperture (NA) objective takes the beam from the lens and focuses it further onto the bundle end. A silica microsphere focuses the exiting NIR beam onto the MCT-A detector. A typical fiber background is shown in Fig. 3 for a mini-bundle of three fibers. With this setup, typical values of energy throughput are: gain = 4, interferogram maximum = 6 for a mini-bundle of three fibers each with  $n = 1.612$ . The signal-to-noise ratio is around 100/1 for the sensors with a 14 cm exposure length.

**Polyisocyanurate Resin.** The spectra of the reacting

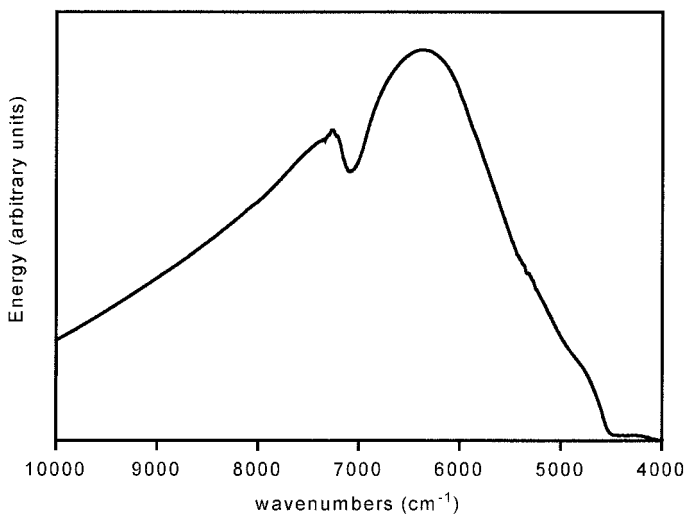


FIG. 3. Single-beam spectrum of fiber-optic mini-bundle.

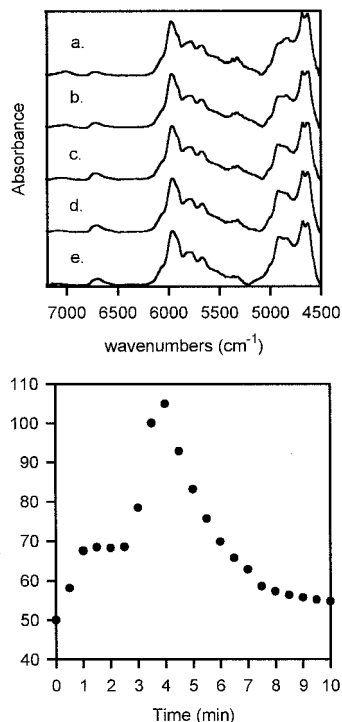


FIG. 4. Spectra of reacting polyisocyanurate resin at (top) 4.44 s (a), 17.8 s (b), 57.8 s (c), 2.97 min (d), and 7.20 min (e). (Bottom) Resin temperature during the reaction.

polyisocyanurate in a 14 cm  $\times$  1 cm  $\times$  1 cm sample cell are shown in Fig. 4 (top). Isocyanurate is a six-membered ring formed from three isocyanate molecules, and a model isocyanurate ring is shown in Fig. 5B. Note the structure in the fiber background and spectrum in the same frequency range (Fig. 3). These spectra are scaled to the internal standard band at 5970  $\text{cm}^{-1}$ , which is an aromatic C-H stretching first overtone.<sup>16</sup> The resin reacts so rapidly that, at 4 s in the sample cell, N-H groups are already forming, as evidenced by the peak formation at 6700  $\text{cm}^{-1}$ . The peak at 6995  $\text{cm}^{-1}$  is an -OH stretching

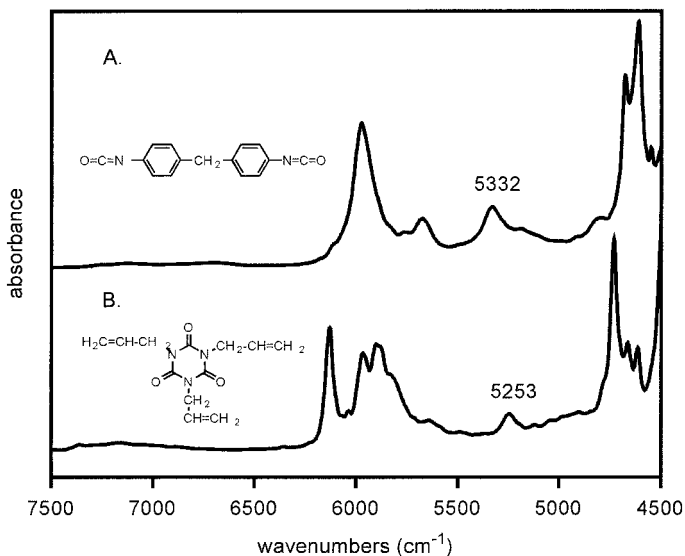


FIG. 5. Spectrum of diphenylmethane diisocyanate (A); spectrum of triallyl-1,3,5-triazine-2,4,6-(1H,3H,5H)trione (B).

**TABLE I. Vibrational assignments for the major polyisocyanurate resin peaks.**

Position (cm <sup>-1</sup> )	Assignment
6995	Hydroxyl stretching overtone
6700	2° Amine overtone
5970	Aromatic -CH stretching overtone
5770	Aliphatic -CH stretching overtone
5673	Aliphatic -CH stretching overtone
5332	Hydrogen-bonded isocyanate -C=O band
5253	Isocyanurate -C=O
5050	Hydrogen-bonded urethane -C=O stretch overtone
4883	2° Amine combination
4870	Hydrogen-bonded urea -C=O stretch overtone
4681	Aromatic -CH stretching combination
4630	Aromatic -CH stretching combination

overtone that is consumed within 1 min. Peaks at 5780 and 5672 are aliphatic -CH stretching overtones. The rather jagged peak at 5332 cm<sup>-1</sup> is the -C=O band<sup>17</sup> of the isocyanate and decreases in intensity with time when compared to the internal standard peak at 5970 cm<sup>-1</sup>. This assignment was confirmed by comparing this spectrum with the spectrum of pure diphenylmethane diisocyanate (MDI) in Fig. 5A.

It can be qualitatively seen from the spectra of the reacting material in the top part of Fig. 4 that the carbonyl peak from the isocyanate is consumed much more slowly than the hydroxyl peak. This is a result of the isocyanate/hydroxyl stoichiometry and catalyst used. There exists an excess of isocyanate groups relative to hydroxyl groups to promote formation of the polyisocyanurate species with the use of the Dabco catalyst. The ratio is 3.5 isocyanate groups/1 polyol group.<sup>18</sup> The formation of the urethane linkage is highly favored at these temperatures and with the Dabco catalyst, and it is because of the nonstoichiometric nature of this reaction that some isocyanurate is formed.<sup>19</sup>

The carbonyl peak from the isocyanurate product should appear at 5253 cm<sup>-1</sup> from the analysis of a model isocyanurate, triallyl-1,3,5-triazine-2,4,6-(1H,3H,5H)trione in Fig. 5B. The exact assignment of this vibrational mode is uncertain, and there is no information in the literature on the NIR assignments of isocyanurate bands. The position of the -C=O stretch is sensitive to hydrogen bonding and temperature and has been used to probe phase separation in polyurethanes.<sup>20</sup> The hydrogen-bonded carbonyl stretch of the urethane linkage appears at 5050 cm<sup>-1</sup> and the -NH combination band at 4883 cm<sup>-1</sup>.<sup>21</sup> The evolution of both the carbonyl peaks from the isocyanurate and the urethane should contribute to the increase of the broad region from 5100 to 4750 cm<sup>-1</sup> in the spectrum. Minor amounts of urea could also contribute to this region, since the urea carbonyl overtone stretching appears at 4870 cm<sup>-1</sup>.<sup>20</sup> The N-H area continues to change throughout the reaction as is seen not only by the well-isolated peak at 6700 cm<sup>-1</sup> but also by the increase in the region around 5000-4800 cm<sup>-1</sup>. The area changes not only are correlated with the amount of -NH present but also should correlate with changes in hydrogen bonding due to temperature effects. Table I summarizes the peak assignments. The competition by polyurethane and iso-

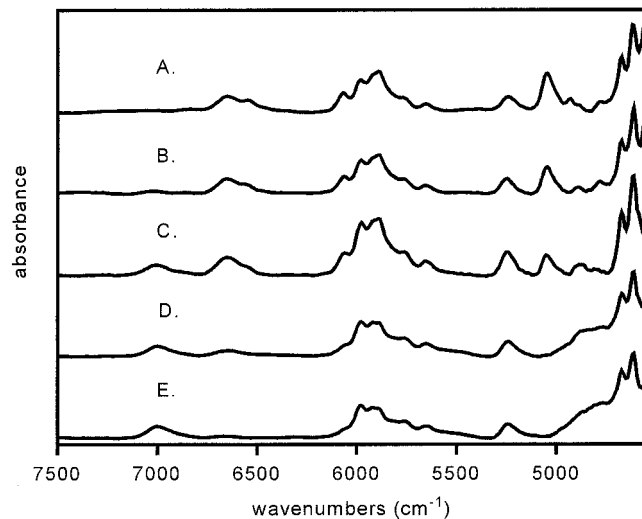


FIG. 6. Spectra of reacting epoxy resin at 0 min, 90 °C (A); 11.4 min, 90 °C (B); 22.0 min, 90 °C (C); 51.5 min, 90 °C (D); 103 min, 115 °C (E).

cyanurate reactions and hydrogen bonding formation may be substantially different at various locations in the part and may affect final part properties.

The lower part of Fig. 4 demonstrates the large exotherm produced by the polyurethane reaction that peaks 58 °C above the initial resin temperature and is significant because of the dependence of heat evolved on resin thickness. Strategically placed mini-bundle sensors could demonstrate the disparity in reaction rate between the composite surface and center of composite thickness due to the difference in temperature between those two places. For the purpose of manufacturing, the polyisocyanurate reaction progresses too rapidly for real-time control. More likely, the spectra can be analyzed off-line, and the mold temperature can be adjusted for future moldings. The isocyanate C=O stretching overtone peak at 5332 cm<sup>-1</sup> and the -OH overtone at 6995 cm<sup>-1</sup> are suitable candidates for off-line monitoring. The choice of a particular peak is dependent upon the time scale of interest, since the total consumption of the -OH group proceeds much faster than that of the -N=C=O group.

**Epoxy Resin.** A liquid molding experiment was performed to successfully demonstrate cure monitoring of an embedded sensor in the center of the mold by using an epoxy resin. The spectra of curing epoxy in the mold as a function of time are shown in Fig. 6. As the resin refractive index increased with cure, the intensity of the internal standard bands increased. Peaks that will be potentially used for analysis of the cure are the primary and secondary amine first overtone at 6650 and 6580 cm<sup>-1</sup>, the aliphatic stretching overtone of the oxirane at 6070 cm<sup>-1</sup>, and the internal standard peak at 5655 cm<sup>-1</sup> that is attributed to the aliphatic -CH overtone.<sup>22</sup> The peak assignments for this resin are summarized in Table II and are similar to other epoxy systems.<sup>23</sup> Cure monitoring and control of a resin transfer molded composite were previously demonstrated with a siloxane preceramic polymer and a surface-mounted mid-infrared sensor.<sup>1</sup>

Figure 7 displays the consumption of the oxirane (6070 cm<sup>-1</sup>), primary and secondary amines (6650 and 6580 cm<sup>-1</sup>), primary amine (5049 cm<sup>-1</sup>), and secondary amine

**TABLE II. Vibrational assignments for the major epoxy peaks.**

Position (cm <sup>-1</sup> )	Assignment
7007	Hydroxyl stretching overtone
6650	1° and 2° Amine stretching overtone
6580	1° Amine stretching overtone
6070	Oxirane -CH stretching overtone
5655	Aliphatic -CH stretching overtone
5242	Liquid water combination
5049	1° Amine combination
4844	Hydroxyl stretching combination
4682	Aromatic -CH stretching combination
4617	Aromatic -CH stretching combination

(calculated) as well as mold temperature. All peak areas were normalized to the internal standard band at 5655 cm<sup>-1</sup>, a methylene overtone band for the conversion calculation. The temperature is that of the mold wall. As is apparent from this figure, all the primary amine is consumed within 40 min, which also corresponds to the maximum in the amount of secondary amine. The conversion of the peaks at 6650 and 6580 cm<sup>-1</sup> represent the combined influences of the primary and secondary amine.

Several peaks would be suitable candidates for real-time spectral analysis. The first would be the primary and secondary amine peaks. The issues associated with these peaks have been discussed above. However, they are well isolated from the rest of the peaks, and areas can be taken directly from the spectrum. The same can be said for the internal standard peak. The oxirane peak exists as a shoulder on a highly overlapping region. The major drawback with attempting to measure areas in real-time is the required modification of the starting and ending points of the peak as the material reacts, which does not lend itself easily to automation. Principal component analysis (PCA) has been shown to be capable of identifying changes in a region of overlapping peaks in near-infrared spectroscopy.<sup>24</sup> With PCA, the spectral region can be chosen to maintain the same starting and ending points for baseline correction throughout the reaction. The region can also be manipulated so that the influence of extraneous peaks can be removed, and the peak of interest can be normalized to an internal standard. PCA can be implemented in the control algorithm and used to represent cure the same way absorbance data are used. For all these reasons, PCA has the potential to be amenable to automation that is required for real-time and off-line data analysis and control.

## CONCLUSION

A high-index fiber-optic mini-bundle evanescent wave sensor has been constructed and interfaced with a near-infrared Fourier transform spectrometer for cure monitoring. Cure monitoring has been demonstrated from 7900 to 4500 cm<sup>-1</sup> for a fast reacting polyisocyanurate resin in a sample cell. The fiber-optic sensor was placed in a mold, and cure monitoring was demonstrated for a

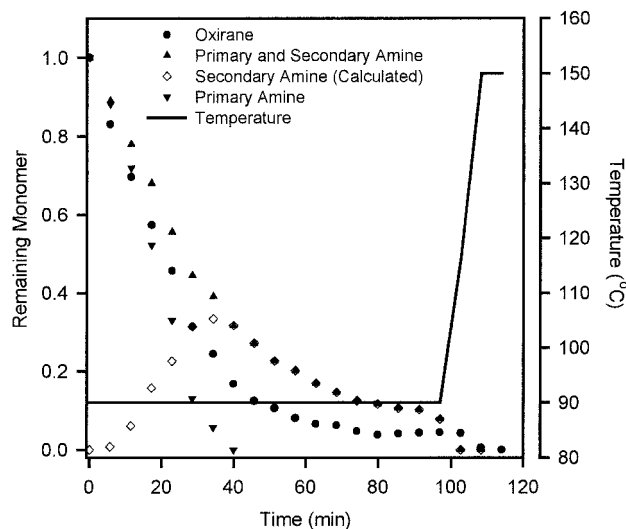


FIG. 7. Plot of remaining oxirane, amine, and temperature.

resin transfer molded epoxy composite part from 10 000 to 4500 cm<sup>-1</sup>. Peak assignments were made and discussed with respect to their potential for use in cure monitoring and control.

1. D. Woerdeman, K. Flynn, J. Dunkers, and R. Parnas, *J. Rein. Plas. and Comp.* **15**, 922 (1996).
2. F. De Thomas, J. Hall, and S. Monfre, *Talanta* **41**, 425 (1994).
3. M. Hansen and A. Khettry, *Polym. Eng. Sci.* **34**, 1758 (1994).
4. H. Chung and M. Arnold, *Appl. Spectrosc.* **49**, 1097 (1995).
5. J. Kirsch and J. Drennan, *Pharm. Res.* **13**, 234 (1996).
6. C. Brown and S.-C. Lo, *Appl. Spectrosc.* **47**, 812 (1993).
7. J. Mijovic and S. Andjelic, *Polymer* **36**, 3783 (1995).
8. G. George, P. Cole-Clarke, N. St. John, and G. Friend, *J. Appl. Polym. Sci.* **42**, 643 (1991).
9. A. Snyder and J. Love, *Optical Waveguide Theory* (Chapman & Hall, London, 1991).
10. S. Cossins, M. Connell, B. Cross, R. Winter, and J. Kellar, *Appl. Spectrosc.* **50**, 900 (1996).
11. D. Woerdeman, K. Flynn, J. Dunkers, and R. Parnas, *J. Rein. Plas. and Comp.* **15**, 922 (1996).
12. J. Dunkers, K. Flynn, and R. Parnas, *Composites, Pt. A.* **28**, 163 (1996).
13. D. Blackburn, Ceramics Division, NIST, private communication (1994).
14. D. Kaufman, Ceramics Division, NIST, private communication (1996).
15. K. Whetsel, *Appl. Spectrosc. Rev.* **2**, 1 (1968).
16. C. Miller, P. Edelman, and B. Ratner, *Appl. Spectrosc.* **44**, 576 (1990).
17. C. Miller and B. Eichinger, *J. Appl. Polym. Sci.* **42**, 2169 (1991).
18. K. Fielder, Dow Chemical Company, Freeport, Texas, personal communication (1997).
19. K. Schwetlick and R. Noack, *J. Chem. Soc., Perkin Trans.* **2**, 395 (1995).
20. C. Miller, P. Edelman, B. Ratner, and B. Eichinger, *Appl. Spectrosc.* **44**, 581 (1990).
21. C. Miller, P. Edelman, and B. Ratner, *Appl. Spectrosc.* **44**, 576 (1990).
22. J. Mijovic and S. Andjelic, *Macromolecules* **28**, 2787 (1995).
23. A. Diaz-Arnold, M. Arnold, and V. Williams, *J. Dent. Res.* **71**, 438 (1992).
24. C. Miller and B. Eichinger, *Appl. Spectrosc.* **44**, 496 (1990).